PHYSICAL REVIEW A **90**, 012707 (2014)

Calculation of the polarization fraction and electron-impact excitation cross section for the Cd^+ $(5p)\,^2P_{3/2}$ state

Christopher J. Bostock,* Dmitry V. Fursa, and Igor Bray
Australian Research Council Centre for Antimatter-Matter Studies, Curtin University, GPO Box U1987, Perth, Western Australia 6845, Australia

Klaus Bartschat†
Australian Research Council Centre for Antimatter-Matter Studies, Curtin University, GPO Box U1987, Perth, Western Australia 6845, Australia and Department of Physics and Astronomy, Drake University, Des Moines, Iowa 50311, USA

(Received 16 June 2014; published 21 July 2014)

We present relativistic convergent close-coupling and Breit-Pauli R-matrix calculations for the polarization of the light emitted after electron-impact excitation of the $(5s)\,^2S_{1/2} \rightarrow (5p)\,^2P_{3/2}$ transition in Cd^+. While we find consistency between the theoretical predictions, a discrepancy persists with the measurements of Goto *et al.* [Phys. Rev. A **27**, 1844 (1983)]. Cascade contributions and hyperfine depolarization effects were calculated and found to have negligible effect on the polarization fraction. We also present angle-integrated cross sections for the $(5p)\,^2P_{3/2}$ state to compare with the measurements of Gomonai [Optc. Spect. **94**, 488 (2003)]. Agreement between theory and experiment is far from perfect, especially at low energies, where they disagree both in the absolute values and the energy dependence of the cross sections.

DOI: 10.1103/PhysRevA.90.012707 PACS number(s): 34.80.Dp

I. INTRODUCTION

The calculation of the light polarization emitted during electron-impact excitation of atoms and ions provides a sensitive test of scattering theories [1]. The fully relativistic convergent close-coupling (RCCC) method [2,3], which is based on the Dirac equation, has been successfully applied to such light-polarization calculations for a range of quasi-one- and two-electron targets [4–8]. More recently the RCCC method has been applied to the calculation of the polarization fraction of the light emitted after electron-impact excitation of the $(6s)\,^2S_{1/2} \rightarrow (6p)\,^2P_{3/2}$ transition in Ba^+ [9]. In that case, a discrepancy between experiment [10] and theory [11] was resolved. Motivated by a similar discrepancy between theory [11] and experiment [12] for the polarization of the light emitted after electron-impact excitation of the Cd^+ $(5s)\,^2S_{1/2} \rightarrow (5p)\,^2P_{3/2}$ transition, we have applied the RCCC method to the case of a Cd^+ ion target. To serve as an independent check of the RCCC results, the Breit-Pauli R-matrix (BPRM) method, which is semirelativistic, was also applied to the problem.

Besides the polarization fraction, we present RCCC and BPRM angle-integrated cross sections for the $(5s)\,^2S_{1/2} \rightarrow (5p)\,^2P_{3/2}$ transition and compare with the measurements of Gomonai [13]. Comparison is also made with the relativistic distorted-wave theory results of Sharma *et al.* [11] and previous 15-state R-matrix calculations of Zatsarinny and Bandurina [14]. We study the manner in which the integrated cross section scales in proportion to the optical oscillator strength for the optically allowed $(5s)\,^2S_{1/2} \rightarrow (5p)\,^2P_{3/2}$ transition. This is relevant because different values appear in the literature for the measured optical oscillator strengths of Cd^+ [15,16]. We provide a generalization of Kim's f-scaling idea [17] for electron-impact excitation cross sections of charged targets.

The next section provides an overview of the RCCC and BPRM theories, and the following section contains results for the polarization fraction and integrated cross sections. Unless indicated otherwise, atomic units are used throughout this paper.

II. THEORIES

A. RCCC method

Comprehensive details of the RCCC method are given in [3] and hence only a brief overview regarding the present application to electron scattering from Cd^+ is given here. The Cd^+ ion is modeled as one active valence electron above a Dirac-Fock $[Kr]4d^{10}$ core. The core orbitals are obtained with the GRASP package [18]. For the Cd^+ valence electron, a set of one-electron orbitals is generated by diagonalization of the quasi-one-electron Dirac-Coulomb Hamiltonian in a relativistic (Sturmian) L-spinor basis [19]. A phenomenological one-electron polarization potential is used to improve the accuracy of the calculated Cd^+ wave functions [20,21]. This allows us to account more accurately for the effect of filled inert shells on the active electrons. The parameters of the polarization potential are adjusted to optimize the target state energies and optical oscillator strengths (OOS). For the one-electron polarization potential we chose the static dipole polarizability of the inert core as $\alpha_d = 4.971$ [22,23] and an l-dependent cutoff parameter $r_c(l)$ with values 2.1, 2.1, 2.0, and 1.9 for $l = 0,1,2,$and 3 respectively.

Our target model consists of 51 states altogether, 34 bound states and 17 continuum states. The energy levels of the first ten states used in the calculations are listed in Table I, and the oscillator strengths for the $(5s)\,^2S_{1/2} \rightarrow (5p)\,^2P_{1/2}$ and $(5s)\,^2S_{1/2} \rightarrow (5p)\,^2P_{3/2}$ resonance transitions are listed in Table II. Core-excited states are neglected in the RCCC

*c.bostock@curtin.edu.au
†klaus.bartschat@drake.edu

TABLE I. Energy levels of the first ten Cd^+ states calculated by diagonalizing the target in the RCCC method. Experimental levels listed by NIST [15] are also shown.

Configuration	RCCC (eV)	Experiment (eV)
$4d^{10}(5s)\ ^2S_{1/2}$	0.00	0.000
$4d^{10}(5p)\ ^2P^\circ_{1/2}$	5.474	5.472
$4d^{10}(5p)\ ^2P^\circ_{3/2}$	5.790	5.780
$4d^{10}(6s)\ ^2S_{1/2}$	10.333	10.299
$4d^{10}(5d)\ ^2D_{3/2}$	11.139	11.120
$4d^{10}(5d)\ ^2D_{5/2}$	11.160	11.139
$4d^{10}(6p)\ ^2P^\circ_{1/2}$	11.767	11.743
$4d^{10}(6p)\ ^2P^\circ_{3/2}$	11.852	11.826
$4d^{10}(7s)\ ^2S_{1/2}$	13.323	13.303
$4d^{10}(4f)\ ^2F^\circ_{5/2}$	13.451	13.442
Ionization limit	16.907	16.908

target structure model for Cd^+ consisting of one valence electron above the frozen Dirac-Fock core. Therefore the states $4d^9(5s^2)\ ^2D_{5/2}$ at 8.587 eV and $4d^9(5s^2)\ ^2D_{3/2}$ at 9.286 eV listed by NIST [15] are missing in Table I.

The target states are used to expand the total wave function of the electron-Cd^+ scattering system and formulate a set of relativistic Lippmann-Schwinger equations for the T-matrix elements. The partial-wave form of the latter equations is

$$T_{fi}^{\Pi J}(k_f\kappa_f,k_i\kappa_i) = V_{fi}^{\Pi J}(k_f\kappa_f,k_i\kappa_i) + \sum_n \sum_\kappa \int\!\!\!\!\!\!\diagup\!\!\!\!\!\!\diagdown dk \times \frac{V_{fn}^{\Pi J}(k_f\kappa_f,k\kappa) T_{ni}^{\Pi J}(k\kappa,k_i\kappa_i)}{E-\epsilon_n^N-\epsilon_{k'}+i0}. \quad (1)$$

The notation in Eq. (1), the matrix elements, and the method of solution using a hybrid OpenMP-MPI parallelization suitable for high-performance supercomputing architectures are given in [3].

In the scattering calculation we add a two-electron (di-electric) polarization potential to model more accurately the interaction of the incident electron with the target. For this potential we again took $\alpha_d = 4.971$, and we set $r^{\rm diel} = 1.7$. This choice of parameters is the same that we used to model the neutral Cd atom [24]. This polarization potential is used to calculate a modified form of the oscillator strength [25,26] for the resonance transitions. As shown in column 3 of Table I this yields good agreement with available experimental values.

As will be seen below, including the two-electron polarization potential in the e-Cd^+ interaction leads to a reduction of the predicted excitation cross sections. For dipole-allowed transitions such a reduction can be understood from the relation between the generalized oscillator strength (GOS) and the differential cross section ($d\sigma/d\Omega$):

$$\mathrm{GOS}(q) = \frac{\Delta E}{2}\frac{p_i}{p_f} q^2 d\sigma/d\Omega. \quad (2)$$

Here q is the momentum transfer; $p_{i,f}$ are the electron momenta before and after the collision, respectively; and ΔE is the excitation energy. At high incident electron energies in the limit $q \to 0$ the GOS converges to the effective optical oscillator strength f. As indicated in the previous paragraph, the value of the effective oscillator strength f should then be obtained using a modified formula for the transition operator [25,26]. It can lead to substantially lower f values that are closer to the experimental results than without inclusion of the dielectronic term. This is indeed the case for the resonance transitions in Cd^+, as seen from column 3 of Table II. The RCCC effective oscillator strength values are close to the recent experimental results (Expt. 1) of Xu *et al.* [16]. Smaller effective oscillator strength values correspond via Eq. (2) to lower angle-differential and ultimately lower angle-integrated cross sections.

The polarization of the light emitted from the $(5p)\ ^2P_{3/2}$ state depends on the magnetic sublevel populations [27,28] according to

$$P = \frac{3(\sigma_{1/2}-\sigma_{3/2})}{3\sigma_{3/2}+5\sigma_{1/2}}, \quad (3)$$

where σ_m is the cross section for excitation to a magnetic sublevel of the $(5p)\ ^2P_{3/2}$ state. The above formula is valid for targets without nuclear spin. Following the procedure outlined by Wolcke *et al.* [29] it should be modified to account for hyperfine-structure depolarization due to admixtures of isotopes with nonzero nuclear spin. We have done this for one set of results presented below, but the effect is too small (less than a 10% reduction in the absolute value of the polarization fraction) to change the predicted physics qualitatively.

Cascades from the high-lying excited levels to the $(5p)\ ^2P_{3/2}$ state can also affect the polarization of the $(5p)\ ^2P_{3/2} \to (5s)\ ^2S_{1/2}$ line. We take into account the cascades by using the method described in [4], but we will demonstrate below that the correction due to this effect is also small.

B. BPRM method

The principal reason for performing these calculations was to provide an independent check of the RCCC predictions. Given that we are interested in an optically allowed resonance transition and the target is a positive ion rather than a neutral atom, channel-coupling effects are expected to be comparatively small, and hence large close-coupling expansions are probably not necessary to obtain accurate results. Furthermore, one would expect the Breit-Pauli approach to be sufficiently

TABLE II. Oscillator strengths of the Cd^+ ground state compared to experimental values listed by NIST [15] and the more recent data of Xu *et al.* [16].

Transition	RCCC	RCCC with 2e pol. pot.	NIST [15]	Expt. [16]
$(5s)\ ^2S_{1/2} \to (5p)\ ^2P_{1/2}$	0.36	0.21	0.23	0.23
$(5s)\ ^2S_{1/2} \to (5p)\ ^2P_{3/2}$	0.76	0.46	0.39	0.55

accurate for the collision problem of interest. Hence, the accuracy of results for e-Cd^+ scattering is to a large extent determined by the accuracy of the target structure description.

In light of the above considerations, we limited the close-coupling expansion to the lowest eight states of Cd^+, once again not counting the core-excited states. As a first step, the core orbitals and a zero-order model potential were generated with the SUPERSTRUCTURE package [30]. Semiempirical potentials to account for core polarization and exchange with the core electrons were then added to the core potential using the program COREPOT [31]. Finally, the one-electron orbitals were recalculated and the potentials were optimized to reproduce the fine-structure-averaged ionization potentials, following the same general ideas as in the RCCC structure calculations described above. The collision calculation was performed with our version of the inner-region Belfast R-matrix codes [32] and the FARM package [33] for the outer region.

III. RESULTS

Figure 1 exhibits the linear polarization fraction of the light emitted after electron-impact excitation of the Cd^+ $(5s)\ ^2S_{1/2} \rightarrow (5p)\ ^2P_{3/2}$ transition. The RCCC results without the two-electron polarization potential (i.e., $\alpha_d = 0$) are shown. We found, however, that the polarization fraction results did not change appreciably when the dielectric term was introduced with $\alpha_d = 4.971$. Also shown in Fig. 1 are the BPRM results with the two-electron polarization potential set to zero. There is excellent agreement with the RCCC results. Hyperfine depolarization of the emitted radiation was then calculated for the BPRM results, and this only had a negligible effect. Both the RCCC and the BPRM polarization fractions are in good agreement with the previous relativistic distorted-wave (RDW) results of Sharma *et al.* [11], except for energies less than about 30 eV, where the RDW results

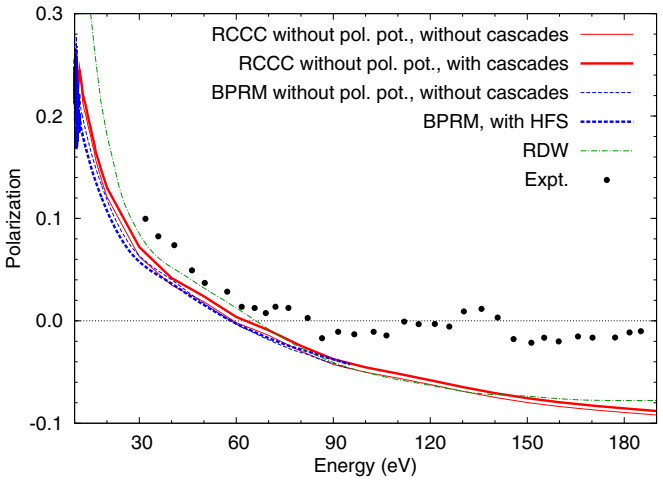

FIG. 1. (Color online) Relativistic convergent close-coupling (RCCC) and Breit-Pauli R-matrix (BPRM) calculations of the polarization fraction with and without cascades for excitation of the $(5s)\ ^2S_{1/2} \rightarrow (5p)\ ^2P_{3/2}$ transition in Cd^+. The measurements are due to Goto *et al.* [12]. The relativistic distorted-wave (RDW) results of Sharma *et al.* [11] are also shown. "BPRM, with HFS" denotes results with hyperfine depolarization taken into account.

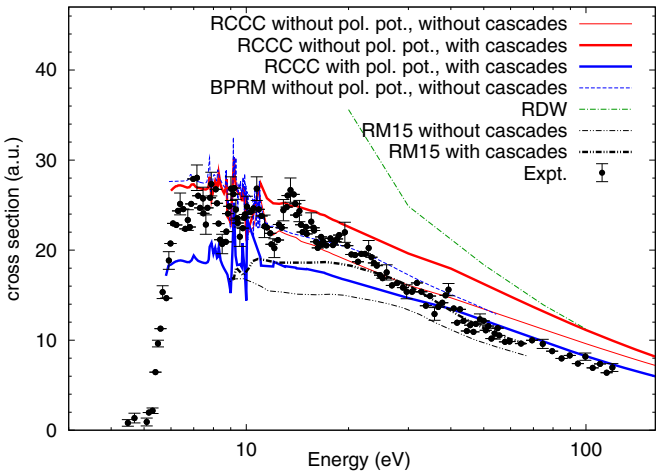

FIG. 2. (Color online) Relativistic convergent close-coupling (RCCC) and Breit-Pauli R-matrix (BPRM) angle-integrated cross sections for the $(5s)\ ^2S_{1/2} \rightarrow (5p)\ ^2P_{3/2}$ transition in Cd^+. The measurements are from Gomonai [13]. The relativistic distorted-wave (RDW) results of Sharma *et al.* [11] and the 15-state R-matrix (RM15) calculations of Zatsarinny and Bandurina [14] are also shown for comparison.

are larger than the other predictions. Given that RDW is most accurate at the higher energies the discrepancy at low energies is expected.

However, there is a discrepancy between all theories and the measurements of Goto *et al.* [12], particularly above 60 eV, where the measurements indicate approximately zero for the polarization fraction. Sharma *et al.* [11] suggested cascades as the most likely reason for the disagreement between their theory and experiment. Consequently, we calculated cascade contributions to the RCCC polarization fraction results. As seen from Fig. 1, however, accounting for the cascades had a negligible effect on the light polarization as well. Upon further analysis of this somewhat surprising result, we found that the two *apparent* (including population by cascades) magnetic sublevel cross sections, $\sigma_{1/2}$ and $\sigma_{3/2}$, are both affected by cascades, but in a way that does not affect Eq. (3) very much (see below).

The RCCC angle-integrated cross section for the Cd^+ $(5s)\ ^2S_{1/2} \rightarrow (5p)\ ^2P_{3/2}$ transition is shown in Fig. 2. For this figure the two-electron polarization potential was set to zero ($\alpha_d = 0$). Results with and without cascade corrections are presented, and we see that cascade effects become appreciable at approximately 10 eV. BPRM results, without cascades, are also illustrated, together with previously published RDW results of Sharma *et al.* [11] and 15-state R-matrix calculations of Zatsarinny and Bandurina [14]. The latter calculations (labeled RM15) were performed in a nonrelativistic framework, but with the inclusion of the core-excited states with principal configurations $3d^9 4s^2$ and $3d^9 4s 4p$. In order to obtain fine-structure-resolved results from this calculation, we multiplied the published $(5s)\ ^2S \rightarrow (5p)\ ^2P$ numbers by the statistical branching ratio of 2/3. The RDW calculations were also multiplied by the same factor because, despite being a relativistic calculation, the published integrated cross section was not fine-structure resolved. The RM15 results are

TABLE III. Magnetic sublevel $\sigma_{m=1/2}$ and $\sigma_{m=3/2}$ cross sections for the $(5s)\ ^2S_{1/2} \rightarrow (5p)\ ^2P_{3/2}$ transition at 190 eV. Cross sections for the direct transition (labeled "dir") are compared with the cascade-corrected cross sections (labeled "cas"). $\sigma_{\rm dir}$ and $\sigma_{\rm cas}$ denote the $(5p)\ ^2P_{3/2}$ integrated cross sections, while P(dir) and P(cas) are the polarization fractions.

Energy (eV)	$\sigma_{\rm dir}$	$\sigma_{\rm cas}$	P(dir)	P(cas)	$\sigma_{1/2,\rm dir}$	$\sigma_{1/2,\rm cas}$	$\sigma_{3/2,\rm dir}$	$\sigma_{3/2,\rm cas}$
190	6.393	7.225	−0.0919	−0.0880	1.410	1.602	1.790	2.015

also shown with and without cascade contributions. In the RM15 calculation, the oscillator strength for the unresolved ^2P level was 0.766, compared to the RCCC value of $0.36 + 0.76 = 1.12$ for the unresolved level without the two-electron polarization potential. The lower RM15 oscillator strength leads to a lower integrated cross section. This is the reason for the discrepancy with the RCCC results at higher energies. However, there is also a different energy dependence seen in the RM15 results compared to the RCCC predictions. This is most likely an indication that coupling to the $4d^9 5s^2$ and $4d^9 5s 5p$ states is somewhat important. For the RDW results of Sharma *et al.* [11], the rapid rise toward lower energies is most likely due to the fact that distorted-wave Born calculations are not unitarized.

Three aspects of the cross-section results deserve attention. First, the measurements of Gomonai [13] exhibit oscillations with intervals of the order of 1 eV. As shown in Fig. 2, these oscillations are not reproduced in any of the theories. Second, cascade contributions have a significant effect, but—as mentioned above—not on the polarization fraction determined from the magnetic sublevel populations via Eq. (3). This indicates that the magnetic sublevel cascade contributions are distributed unevenly (polarized) between the $\sigma_{m=1/2}$ and $\sigma_{m=3/2}$ magnetic sublevels. Table III illustrates a sample of explicit magnetic sublevel results at 190 eV, with and without cascade corrections, and the corresponding polarization fraction and integrated cross section. It is apparent that cascades, on a percentage basis, affect the $\sigma_{m=1/2}$ more than the $\sigma_{m=3/2}$ level. The overall effect is a negligible change to the polarization fraction when cascade corrections are included.

The third important aspect of the theoretical cross section is the fact that it, unlike the polarization fraction, scales in proportion to the optical oscillator strength of the respective transition in the target. This is illustrated in Fig. 3, which exhibits the RCCC results with $\alpha_{\rm d} = 4.971$ for the two-electron polarization potential. The predicted cross sections, like the optical oscillator strengths in Table II, are substantially lower when $\alpha_{\rm d} = 4.971$ is employed. However, when the $\alpha_{\rm d} = 0$ results (i.e., without the polarization potential) are rescaled by the ratio of the optical oscillator strengths, the curves lie practically on top of each other. The same holds for the BSRM calculations (not shown in Fig. 3). Therefore, for target models in which the polarization potential parameters can be adjusted to obtain improved oscillator strengths, the adjustment scales the integrated cross section in proportion.

Going even further, if the collision part of a calculation is likely converged with the number of coupled states, but some aspects of the target structure are not sufficiently accurate, rescaling with the ratio of the preferred oscillator strength and the theoretical value should improve the result over the *entire energy range*. This is a generalization of Kim's f-scaling idea [17], since it does *not* require an *ad hoc* shift of first-order Born results in the intermediate energy regime. In Kim's method, the relativistic Coulomb-Born cross section is multiplied by the ratio $T/(T + E)$, where T is the energy of the projectile and E is the excitation energy, and then further multiplied by the ratio of the preferred oscillator strength to the theoretical value (0.46 to 0.76). Figure 3 illustrates results generated with this method (denoted "Ef-scaled"); agreement with the scaled RCCC results is quite remarkable. We note that historically Kim's f-scaling idea can be traced back to Van Regemorter [34] and that modelers in astrophysics have been rescaling dipole collision strengths based on better f-value structure results for a long time, out of necessity to resolve discrepancies between theory and observation for intensity ratios. An example is Del Zanna [35], who rescaled the dipole collision strengths (at all energies) of Griffin *et al.* [36]. Indeed, Griffin *et al.* noted that their key diagnostic dipole collision strengths were likely to be reduced by the same percentage as that of their best f values (which could not be used in the collision calculation).

Figure 3 also includes a comparison with the RM15 results of Zatsarinny and Bandurina [14], which we scaled by the ratio of the optical oscillator strength (present: 0.46, RM15: 0.51) to guarantee the same high-energy behavior. The differences between the scaled RCCC and RM15 results at low and

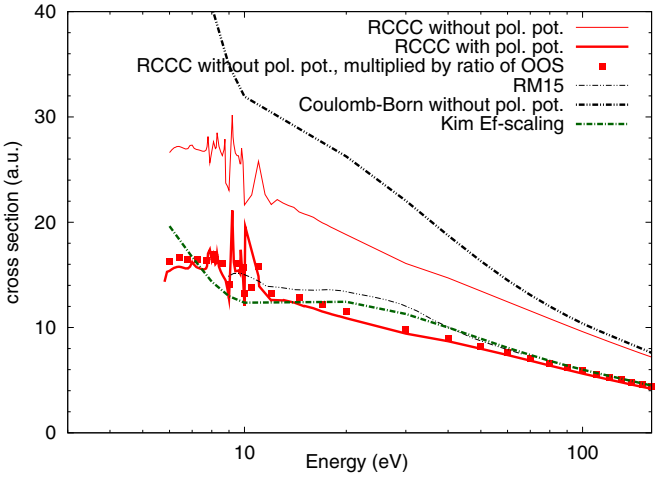

FIG. 3. (Color online) Relativistic convergent close-coupling (RCCC) and Coulomb-Born calculations of angle-integrated cross sections for the $(5s)\ ^2S_{1/2} \rightarrow (5p)\ ^2P_{3/2}$ transition in Cd^+. Also shown are 15-state R-matrix (RM15) results of Zatsarinny and Bandurina [14] and Kim's [17] Ef-scaled results. The latter results are described in the text and are obtained from scaled Coulomb-Born results. All the results presented in this figure are direct cross sections without cascade corrections.

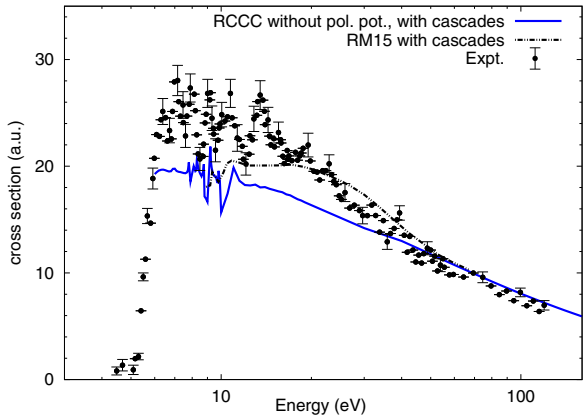

FIG. 4. (Color online) Relativistic convergent close-coupling (RCCC) and 15-state R-matrix (RM15) calculations of Zatsarinny and Bandurina [14] of the angle-integrated cross section for the $(5s)\ ^2S_{1/2} \rightarrow (5p)\ ^2P_{3/2}$ transition in Cd^+. The measurements are from Gomonai [13].

intermediate energies are likely an indication of the coupling to the core-excited states that is included in the RM15 model but is missing in RCCC model.

Any inaccuracy in the description of the target wave functions will inadvertently lead to a corresponding inaccuracy in the predicted excitation cross sections. For dipole-allowed transitions the theoretical cross sections can be corrected by scaling with the ratio of optical oscillator strengths if a reliable value of the oscillator strength for the transition of interest is available. In Fig. 4 we present our best estimate for the excitation cross sections by scaling the RCCC cross sections (with cascades, without polarization potential); i.e., we multiplied the RCCC cross section by the ratio of the experimental optical oscillator strength value [16] (0.55) to the present RCCC value (0.76). The RM15 results (with cascades) are also presented and similarly rescaled with the ratio of oscillator strength (0.55 to 0.51). The agreement between theory and experiment is good at high energies, whereas at energies below 30 eV the theoretical results are consistently lower than experiment. While our RCCC and BSRM calculations do show a resonance behavior at low energies, the details disagree with the resonance behavior observed in the experiment.

IV. CONCLUSION

RCCC and BPRM calculations for the polarization fraction of the light emitted after electron-impact excitation of the $(5s)\ ^2S_{1/2} \rightarrow (5p)\ ^2P_{3/2}$ transition in Cd^+ are in agreement with the RDW calculations of Sharma *et al.* [11] but in disagreement with the measurements of Goto *et al.* [12], particularly above 60 eV. Cascade contributions are found to have a negligible affect on the polarization fraction due to the fact that the magnetic sublevel cascade contributions are distributed unevenly between the $\sigma_{m=1/2}$ and $\sigma_{m=3/2}$ magnetic sublevels. We also found that hyperfine depolarization effects are negligible. For the cross section of the $(5p)\ ^2P_{3/2}$ state we find good agreement with the measurements of [13] only at relatively large energies (above 30 eV). At lower energies the theoretical results are lower than experiment and the theories do not reproduce the oscillations in the energy dependence. We found that cascade contributions have a significant effect on the predicted cross section and that the latter scales in proportion to the optical oscillator strength.

ACKNOWLEDGMENTS

Support of the Australian Research Council and Curtin University is acknowledged. We are grateful for access to the Australian National Computational Infrastructure and its Western Australian node iVEC. K.B. would like to acknowledge financial support from the United States National Science Foundation under Grant No. PHY-1068140 and the hospitality of Curtin University.

[1] N. Andersen and K. Bartschat, *Polarization, Alignment, and Orientation in Atomic Collisions* (Springer, New York, 2000).
[2] D. V. Fursa and I. Bray, Phys. Rev. Lett. **100**, 113201 (2008).
[3] C. J. Bostock, J. Phys. B **44**, 083001 (2011).
[4] C. J. Bostock, D. V. Fursa, and I. Bray, Phys. Rev. A **80**, 052708 (2009).
[5] C. J. Bostock, D. V. Fursa, and I. Bray, Phys. Rev. A **83**, 052710 (2011).
[6] M. J. Berrington, C. J. Bostock, D. V. Fursa, I. Bray, R. P. McEachran, and A. D. Stauffer, Phys. Rev. A **85**, 042708 (2012).
[7] C. J. Bostock, D. V. Fursa, and I. Bray, Phys. Rev. A **88**, 062707 (2013).
[8] C. J. Bostock, D. V. Fursa, and I. Bray, Phys. Rev. A **89**, 032712 (2014).
[9] C. J. Bostock, D. V. Fursa, and I. Bray, Phys. Rev. A **89**, 062710 (2014).
[10] D. H. Crandall, P. O. Taylor, and G. H. Dunn, Phys. Rev. A **10**, 141 (1974).
[11] L. Sharma, A. Surzhykov, R. Srivastava, and S. Fritzsche, Phys. Rev. A **83**, 062701 (2011).
[12] T. Goto, K. Hane, M. Okuda, and S. Hattori, Phys. Rev. A **27**, 1844 (1983).
[13] A. Gomonai, Optics and Spectroscopy **94**, 488 (2003).
[14] O. I. Zatsarinny and L. A. Bandurina, Optics and Spectroscopy **89**, 488 (2000).
[15] http://physics.nist.gov/PhysRefData/ASD/levels_form.html.
[16] H. L. Xu, A. Persson, S. Svanberg, K. Blagoev, G. Malcheva, V. Pentchev, E. Biémont, J. Campos, M. Ortiz, and R. Mayo, Phys. Rev. A **70**, 042508 (2004).
[17] Y.-K. Kim, Phys. Rev. A **65**, 022705 (2002).
[18] K. G. Dyall, I. P. Grant, C. T. Johnson, F. P. Parpia, and E. P. Plummer, Comp. Phys. Comm. **55**, 425 (1989).
[19] I. P. Grant and H. M. Quiney, Phys. Rev. A **62**, 022508 (2000).
[20] D. V. Fursa and I. Bray, J. Phys. B **30**, 5895 (1997).

[21] D. V. Fursa, I. Bray, and G. Lister, J. Phys. B **36**, 4255 (2003).
[22] W. R. Johnson, D. Kolb, and K. N. Huang, At. Data Nucl. Data Tables **28**, 333 (1983).
[23] A. Ye and G. Wang, Phys. Rev. A **78**, 014502 (2008).
[24] C. J. Bostock, M. J. Berrington, D. V. Fursa, and I. Bray, Phys. Rev. Lett. **107**, 093202 (2011).
[25] S. Hameed, A. Herzenberg, and M. G. James, J. Phys. B **1**, 822 (1968).
[26] C. Laughlin and G. A. Victor, in *Atomic Physics*, edited by S. J. Smith and G. K. Walters (Plenum, New York, 1972), Vol. 3, p. 247.
[27] E. G. Berezhko and N. M. Kabachnik, J. Phys. B **10**, 2467 (1977).
[28] K. J. Reed and M. H. Chen, Phys. Rev. A **48**, 3644 (1993).
[29] A. Wolcke, K. Bartschat, K. Blum, H. Borgmann, G. F. Hanne, and J. Kessler, J. Phys. B **16**, 639 (1983).
[30] W. Eissner, M. Jones, and H. Nussbaumer, Comput. Phys. Commun. **8**, 270 (1974).
[31] K. Bartschat, in *Computational Atomic Physics*, edited by K. Bartschat (Springer, Heidelberg, 1996).
[32] K. A. Berrington, W. B. Eissner, and P. H. Norrington, Comp. Phys. Comm. **92**, 290 (1995).
[33] V. M. Burke and C. J. Noble, Comp. Phys. Comm. **85**, 471 (1995).
[34] H. Van Regemorter, Astrophys. J. **136**, 906 (1962).
[35] G. Del Zanna, Astron. Astrophys. **508**, 513 (2009).
[36] D. Griffin, M. Pindzola, and N. Badnell, Astron. Astrophys. Suppl. Ser. **142**, 317 (2000).